Volume distributions of avalanches in lung inflation: A statistical mechanical approach

Mamatha K. Sujeer,[1] Sergey V. Buldyrev,[2] Stefano Zapperi,[2] José S. Andrade, Jr.,[3] H. Eugene Stanley,[2] and Béla Suki[1]
[1]*Department of Biomedical Engineering, Boston University, Boston, Massachusetts 02215*
[2]*Department of Physics, Center for Polymer Studies, Boston University, Boston, Massachusetts 02215*
[3]*Departamento de Física, Universidade Federal do Ceará, 60451-970 Fortaleza, Ceará, Brazil*
(Received 6 February 1997)

To study the dynamics of lung inflation, we introduce a statistical mechanical model that incorporates experimental observations that, during lung inflation from low volumes, (i) each individual airway segment opens when the external inflation pressure reaches a critical opening threshold corresponding to that segment and (ii) airway opening in the lung occurs in cascades or by avalanches. The model includes realistic asymmetry of the bronchial tree, tissue elasticity, and airway and alveolar dimensions. We perform numerical simulations of lung inflation to study the effects of these attributes on the volume distributions of both the *first* and *all* avalanches for three different distributions of critical opening threshold pressures: (a) a generation-independent, (b) a slightly generation-dependent, and (c) a highly generation-dependent distribution. For both the first and all avalanches we find that the volume distribution is a power law, except for the highly generation-dependent threshold distribution. Asymmetry and realistic airway and alveolar dimensions slightly modify the scaling region, but retain a power-law behavior as long as the distribution of threshold pressures is *generation independent* or slightly generation dependent. Also, for such a distribution of threshold pressures, the scaling exponent of the most realistic model (the asymmetric tree with realistic airway and alveolar dimensions and tissue elasticity) is 2, which is the value obtained both analytically using percolation theory and from simulations on a Cayley tree. Thus the power-law behavior and the scaling exponents are a consequence of finite-size effects and a distribution of threshold pressures that is generation independent or slightly generation dependent. We also predict the pressure-volume relationship of the model, which is easily and noninvasively accessible in clinical settings. The results of the avalanche size distributions and pressure-volume curves support the notion that at low lung volumes, the distribution of the critical opening threshold pressures in the normal lung is most likely wide with negligible generational dependence.
[S1063-651X(97)05708-5]

PACS number(s): 87.45.−k

I. INTRODUCTION

The dynamics of a vast class of driven disordered systems takes place in avalanches of broadly distributed sizes. Examples include the motion of domain walls in disordered ferromagnets [1], flux lines in superconductors [2], fluid flow through porous media [3], microfracturing processes [4], and earthquakes [5]. The common feature of these apparently very different phenomena lies in the presence of a slowly increasing external force competing with quenched disorder that tends to hinder the dynamics.

Avalanche dynamics has been observed in the inflation of degassed lungs [6], a problem that may have important physiological implications. During a forced exhalation, lungs deflate to very low volumes. As a result of local instabilities, many peripheral airways close up [7]. In lung disease, closure occurs even during normal breathing. If the closed airways do not reopen for a significant portion of the following inhalation, large portions in the alveolar space can remain closed during the entire breathing cycle, leading to severe hypoventilation and imbalance between ventilation and perfusion [8]. Thus it is important to understand how airways reopen.

The process of opening a single airway is a local and isolated phenomenon. However, the dynamics of consecutive airway openings in the lungs is a highly cooperative process. There is experimental evidence suggesting that during inflation, the resistance to airflow of the small airways decreases in discrete jumps due to the fact that opening of an airway requires the overcoming of a critical opening threshold pressure at the site of closure [9,10]. To interpret these data, it was shown that airways do not open individually, but in a sequence of bursts or ''avalanches'' involving many airways; both the size of these jumps and the time intervals between the jumps follow power-law distributions [6]. In this context, the inhomogeneities in the opening threshold pressures provide a form of quenched disorder that obstruct the flow of air. The competition between the increasing external air pressure and the local thresholds gives rise to the observed avalanche behavior.

Apart from the physiological implications of the problem, lung inflation takes place in a hierarchical structure, which greatly simplifies the theoretical analysis of the phenomenon. This is in contrast with many other avalanche phenomena for which a satisfactory theory is usually not available. Recently, the problem was mapped into a percolation model on a Cayley tree, with the inflated lung volume corresponding to a percolation cluster, which allowed the analytical derivation of the exponents describing the size distributions of the first avalanche [11]. These results were also tested using numerical simulations of lung inflation on a statistical mechanical model of the airway tree [11].

The model of Ref. [11] is, however, highly simplified compared to the actual airway structure of the lung. Specifi-

cally, the airways are assumed to be rigid and of the same dimensions for all airway segments constituting a symmetric binary tree. Further, this model is used to study the size distributions of only the first avalanche that occurs during lung inflation. Finally, and most importantly, in the model of Ref. [11], the critical opening threshold pressures are assumed to be uniformly distributed throughout the tree. However, according to some recent experimental observations, the opening threshold pressures in the lung appear to decrease with increasing airway dimensions [12].

In this paper, we extend the model introduced in [11] to a more realistic representation of the airway structure in the lung. First, using a stochastic design principle of the bronchial tree [13], we introduce realistic asymmetric trees, defined as symmetric binary trees with some branches missing. The airways are then assigned lengths and diameters according to actual morphometric data. To distinguish between the tree with all its airways having the same dimensions and the tree with realistic airway dimensions, we call the former tree ''normalized'' and the latter ''unnormalized.'' The limitation of rigid airway walls is also removed by requiring that the diameter of each airway (and therefore the volume) is a function of the pressure in that airway. We investigate extensively the issue of the generation-dependent distribution of opening threshold pressures by performing simulations for three different distributions of threshold pressures: (a) a generation-independent, (b) a slightly generation-dependent, and (c) a highly generation-dependent distribution of threshold pressures. As in the model of Ref. [11], two definitions of the ''size'' of an avalanche are considered separately. We use the model described in this paper to study the size distributions of not only the first avalanche, but of all avalanches. Our results support the notion that in the normal lung at low volumes, the distribution of the opening threshold pressures is not essentially different from a generation-independent distribution and suggest implications for ventilation strategies for individuals suffering from significant airway closure and/or alveolar collapse.

II. MODEL FORMULATION

A. Symmetric binary tree

According to morphological data [14], the human (as well as other mammalian) lung is an asymmetric branching airway structure with approximately 35 generations. Complete airway closure on exhalation appears to occur only in the last approximately 10–14 generations [6], where the branching is reasonably symmetric [14]. Accordingly, as a first step, this part of the airway tree is a 12-generation symmetric binary Cayley tree with airway segments that can be either closed or opened. At time $t=0$, all airways are assumed to be closed. Lung inflation is simulated by applying an external pressure P_E at the top of the tree and gradually increasing P_E at a slow rate [11].

Airways are labeled (i,j) with a generation number i ($i=0,\ldots,N$), where N is the order of the tree ($i=0$ denotes the root of the tree: the trachea), and a column number j ($j=0,\ldots,2^i-1$). Experiments on flexible tube airway models [15] show that the opening of a single airway is a dynamic process, with each airway characterized by a critical pressure threshold such that if P_E exceeds this threshold, then the airway opens. Thus, in the model, an opening threshold pressure $P_{i,j}$ is assigned to each airway (i,j), which ''pop'' open instantaneously whenever $P_{i,j}$ is smaller than or equal to the pressure in its parent [6,11].

The inflation of the lung model is simulated by increasing P_E in small increments. P_E is initially assigned the value $P_{0,0}$, the critical threshold pressure of airway (0,0). Since an airway opens when the pressure in its parent equals or exceeds its critical threshold pressure, the airway (0,0) now opens and its pressure is set equal to P_E. Next, the two airways (1,0) and (1,1) are tested to see if they can be opened by this value of P_E (the current pressure in their parent airway), i.e., whether $P_E \geqslant P_{1,0}$ and/or $P_E \geqslant P_{1,1}$. If one or both conditions are met, then the airways (1,0) and/or (1,1) are also opened. This opening is then continued sequentially down the tree until no airway is found with $P_{i,j} \leqslant P_E$. Of particular interest is the fact that a small increase in P_E can lead to an ''avalanche'' in which many airways open simultaneously [16]. When the first avalanche stops, the threshold pressures of those airways that are still closed but whose parents are now open are examined. P_E is incremented to the smallest of these threshold pressures and the pressure in the open airways is updated to this new value. This process is iterated until all airways open. The location and size of the next avalanche depends on the distribution of $P_{i,j}$ in the accessible region.

Two definitions of the size of an avalanche are considered. In definition A, since gas exchange in the lung occurs only in the ''open'' alveoli (the 2^N terminal units of the bronchial tree) that are in communication with the trachea, v denotes the total volume of all those alveoli that become connected to the root by the avalanche [17]. In definition B, motivated by percolation theory [18,19], s is the number of airways that open following an increase of P_E that opens at least one airway.

B. Asymmetric binary tree

The next step toward a more realistic airway tree involves introducing asymmetry. We create asymmetric branching using the design method of [13], which is based on stochastic flow divisions at bifurcations. Briefly, the motivation for this is that the airway tree is primarily a branching ductal structure designed for the purpose of efficient fluid transportation. The flow Q starts at the top of the airway structure, dividing itself at each bifurcation, until it reaches the terminal branches where the flow dividing process stops and the fluid is delivered to the terminal units of the tree called the acini. Although there is further branching within an acinus, the acinus is defined as the functional unit for gas exchange because the respiratory bronchioles are no longer pure conductive ducts. Accordingly, there is a threshold flow rate Q_c below which there is no more conductive flow division. Thus Q_c provides the maximum flow rate at the terminal branches. The flow rate at the top of the tree is assigned to be unity. The flow rate before branching Q_0 (i.e., the flow rate of the parent) is equal to the sum of the flow rates of the two daughter branches (Q_1 and Q_2 with $Q_1 \geqslant Q_2$ by convention). The flow dividing ratio is defined as $r=Q_2/Q_0$ ($0 \leqslant r \leqslant 0.5$) so that $Q_1/Q_0=1-r$. The ratio r is regarded as a random variable. Thus, starting from the root, the flow rate is

divided at each bifurcation with a ratio r until the threshold flow rate Q_c is reached. The airways with flow rates less than Q_c are taken to be part of the alveoli [13]. This algorithm completely defines the topology of the tree. When r is fixed to 0.5, the flow division is completely symmetric, resulting in a symmetric tree. For the 12-generation tree model used in this study, a uniform distribution of r between 0.1 and 0.3 and a Q_c of 0.0002 yield an asymmetric tree with a number of airways approximately one-third of that in a corresponding 12-generation symmetric tree.

C. Symmetric and asymmetric trees with realistic dimensions from morphometric data

Next, the tree is resized by modeling each airway as a cylindrical tube, with lengths and radii obtained from a model of the rat lung described by Yeh, Schum, and Duggan [20]. In this airway model, which was based on the complete data set for the conducting airways measured by Raabe *et al.* [21], airway diameter decreases with increasing generation number by a factor ~7. Thus, instead of the number of segments opened, the size of an avalanche is now measured in terms of the absolute *volume* of the newly recruited airways constituting an avalanche rather than the *number* of opened airways. Thus, for definition B, s is the total volume of all the airways that make up an avalanche. For definition A, since all alveoli have the same volume, the size of an avalanche v is still simply the number of alveoli opened following an avalanche.

D. Tissue elasticity

Elasticity is introduced into the present model by requiring that the diameters (and therefore the volumes) of the opened airways and alveoli depend on the external pressure. These diameter values are updated with each increase in pressure according to a single exponential diameter-pressure relationship taken from the literature [22,23]. Thus a newly opened airway or alveolus will ''distend'' due to the elastic nature of its wall to a volume that is a function of P_E and so contribute to an avalanche with a volume greater than that of a corresponding airway or alveolus from a rigid tree for the same value of P_E. For trees with realistic dimensions (with and without elasticity), the avalanche volumes were normalized such that the smallest possible avalanche is assigned a unit volume. The equation describing the P_E-airway volume is

$$s = \pi l r^2, \tag{1}$$

where

$$r = r_0\{1 + 0.2[1 - \exp(-4P_E)]\}. \tag{2}$$

Here s is the airway volume at P_E, l is the airway length, r is the airway radius at P_E, and r_0 is the end-expiratory airway radius. The P_E-alveolar volume relationship is

$$v = v_0\{1 + 4[1 - \exp(-4P_E)]\}, \tag{3}$$

where v is the volume of a single alveolus at P_E and v_0 the end-expiratory alveolus volume.

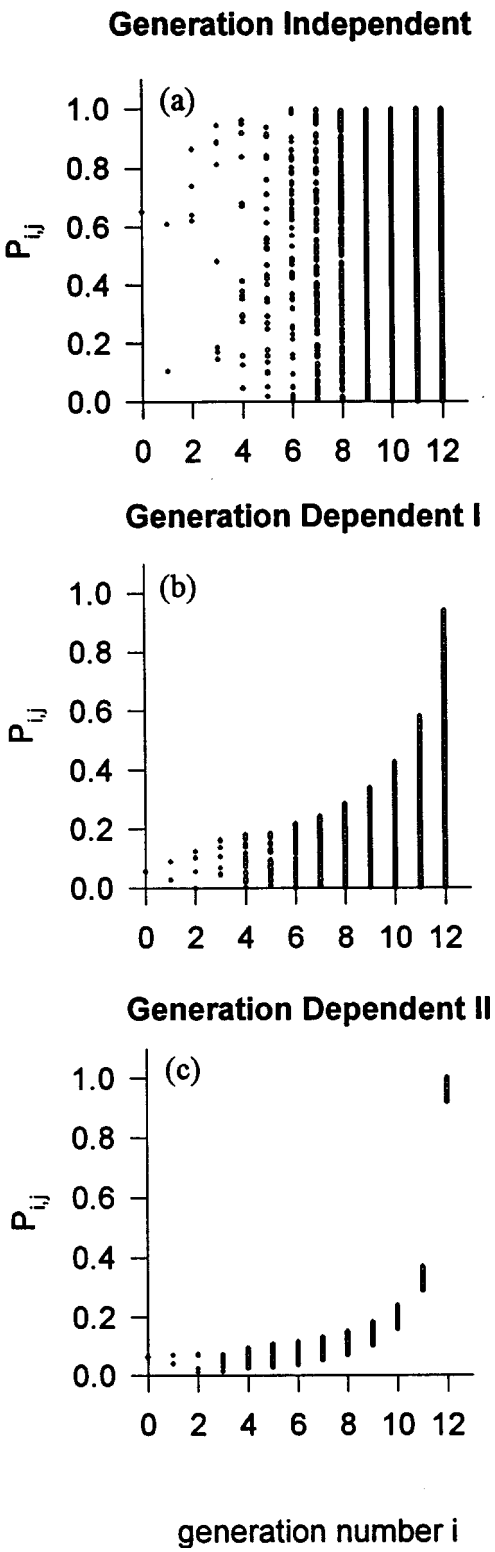

FIG. 1. Single representative realization of each of the three distributions of normalized threshold pressures $P_{i,j}$ with generation number: (a) generation independent, $P_{i,j}$ distributed uniformly between 0 and 1 for all generations; (b) generation-dependent I, $P_{i,j}$ distributed in small intervals with the lower end of the intervals extending down to 0 and the upper ends falling along a hyperbolic curve as a function of generation number; (c) generation-dependent II, $P_{i,j}$ distributed in small intervals with both ends of the intervals falling along a hyperbolic curve as a function of generation number.

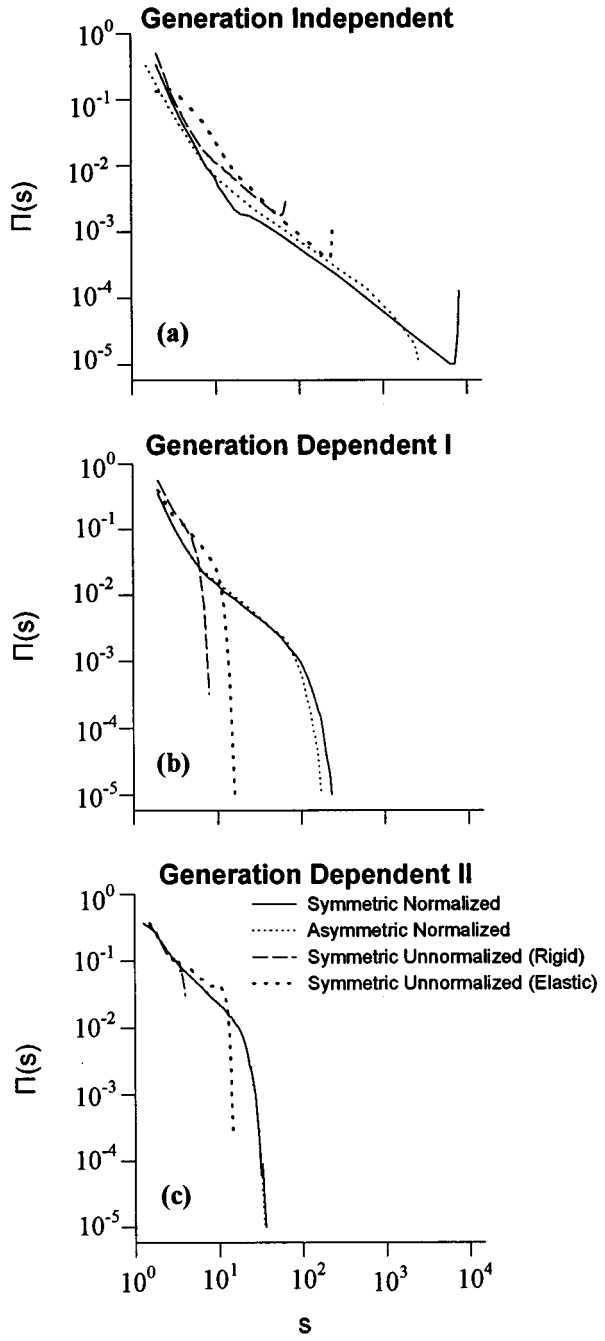

FIG. 2. Double logarithmic plots of the size distributions $\Pi(s)$ of the first avalanches for all three distributions of $P_{i,j}$, obtained by computer simulations on a Cayley tree of 12 generations for definition *B* (airways). The solid line is the size distribution for the symmetric tree. The dotted line represents the asymmetric tree, which is essentially a symmetric tree with some of its branches missing. The dashed line is the symmetric tree with realistic diameters and lengths taken from morphometric data (unnormalized). The bold-dotted line represents the symmetric, unnormalized tree with compliant airway walls.

E. Opening threshold pressure distributions

In order to investigate the influence of the distribution of $P_{i,j}$ on the scaling behavior of avalanche sizes, three different distributions are used to calculate the distributions of s and v for all the models described above (Fig. 1). The generation-independent distribution [Fig. 1(a)] requires $P_{i,j}$ to be uniformly distributed between 0 and 1 for all generations. The basis for this choice is that we found that a generation-independent distribution provides excellent quantitative agreement with the distribution of the terminal airway resistance jumps that were determined from experimental data [6]. Generation-dependent distributions I and II are generated based on the limited data of initial opening threshold pressures in isolated lungs as a function of airway radius measured recently by Naureckas *et al.* [12]. For the generation-dependent I distribution [Fig. 1(b)], $P_{i,j}$ is distributed in small intervals with the lower ends of each interval extending to zero and the upper ends falling along a hyperbolic curve as a function of increasing generation number, i.e., for the ith generation, the threshold pressures are distributed uniformly in the interval

$$\left[0, \frac{0.1N}{N-0.88i}+0.04\right], \quad i=0,1,2,\ldots,N. \tag{4}$$

The generation-dependent II distribution [Fig. 1(c)] is the same as the generation-dependent I distribution except that the lower ends of the interval also fall along a hyperbolic curve, i.e., for the ith generation, the threshold pressures are distributed as

$$\left[\frac{0.1N}{N-0.88i}-0.04, \frac{0.1N}{N-0.88i}+0.04\right], \quad i=0,1,2,\ldots,N. \tag{5}$$

Generation-dependent distributions I and II both show a generational dependence of $P_{i,j}$ in that the mean of $P_{i,j}$ increases with increasing I.

F. Simulations

For the first avalanches, we simulate lung inflation a sufficient number of times to obtain 100 000 first avalanche size values. In order to compare avalanche size distributions for different cases, it is important that all data are binned similarly, since bin sizes can significantly influence the shapes and therefore the exponents of the curves. For all avalanches, 5000 simulations of lung inflation are performed for each case. We choose a uniform binning of size one. The probability distribution functions obtained from the binning of data are then displayed on a double logarithmic plot. The slopes of the scaling regions are calculated by considering only the linear portions of the curves. The error bars for each of these slopes are calculated as follows. First, the slope of the linear portion of the curve is calculated as α. This portion of the curve is now divided into two halves and the slopes for each half calculated as α_1 and α_2, respectively. The error bars for α are then $\pm(\alpha_1-\alpha_2)$.

III. RESULTS AND DISCUSSION

A. First avalanche: Definition *B*

1. Normalized symmetric and asymmetric

For simplicity we begin with definition *B*. Figure 2 shows on a double logarithmic plot the size distributions $\Pi(s)$ of

TABLE I. Scaling exponents of the size distributions $\Pi(s)$ of the first avalanches for definition *B* (airways) using all three distributions of $P_{i,j}$. The two scaling exponents for all distributions that show two distinct scaling regions are shown in the table separated by a comma. The first value represents the upper scaling region (see the text) and the other the lower scaling region.

	Normalized		Unnormalized (rigid)		Unnormalized (elastic)	
$P_{i,j}$	Symmetric	Asymmetric	Symmetric	Asymmetric	Symmetric	Asymmetric
Generation-independent	2.1±0.2, 1.0±0.1	2.0±0.2, 1.0±0.1	2.1±0.3, 1.1±0.1	2.1±0.3, 1.1±0.3	1.9±0.3, 1.1±0.2	1.9±0.3, 1.1±0.2
Generation-dependent I	2.2±0.2, 1.0±0.1	2.2±0.2, 1.0±0.1	2.2±0.3	2.2±0.3	2.2±0.1, 1.3±0.3	2.2±0.1, 1.3±0.3
Generation-dependent II						

the first avalanches for the three distributions of $P_{i,j}$. Here we compare symmetric and asymmetric trees when they are normalized, that is, when they are assigned physiological dimensions with and without elasticity. For the generation-independent distribution of $P_{i,j}$ [Fig. 2(a)], the simulation results show that $\Pi(s)$ has two distinct scaling regions: an upper region with a steep power-law decay with an exponent of ~2.0 and a second, lower region with a moderate power-law decay with an exponent of ~1.0. The crossover occurs at a size of N (N is the number of generations, which is 12 in this study). Also there is a ''kink'' in $\Pi(s)$ at large s. These features are in agreement with previous analytical results based on percolation theory [11].

Table I summarizes the exponents calculated in the two scaling regions for all cases considered. It can be seen from Fig. 2(a) and Table I that in a normalized rigid tree, asymmetry has a negligible effect on $\Pi(s)$: both the power-law behavior and the exponents are the same for all three $P_{i,j}$ distributions. However, asymmetry causes the scaling region to be slightly reduced with the crossover shifting to the left. We can explain this if we consider the asymmetric tree as a symmetric binary tree with some branches missing. Asymmetry does maintain treelike connectivity, which is necessary for power-law behavior. Also, since all airways in the asymmetric tree are assumed to be identical, the scaling exponents are similar to those of the symmetric tree. The scaling regions, however, depend on the size of the tree. In the present model, we start with a symmetric 12-generation tree and then introduce asymmetry by removing some branches from the tree as described in Sec. II. Consequently, the ''size'' of the airway tree is smaller than that of a symmetric tree. Hence the crossover in an asymmetric tree (built from a 12-generation symmetric tree) occurs at a generation number less than 12. The decreased scaling regions are thus a consequence of the reduced number of airways in the asymmetric tree.

2. Assigning realistic airway dimensions and elasticity

Figure 2 also shows the effect on $\Pi(s)$ of introducing realistic dimensions and elasticity. Assigning realistic lengths and diameters to the tree (with the airways normalized so that the trachea has a unit volume) does not affect the shape of $\Pi(s)$, i.e., the power-law behavior is not destroyed since the treelike connectivity of the airways is preserved. There is, however, a reduction in the scaling regions due to the fact that airway dimensions decrease with increasing generation number, so the newly recruited volume for each avalanche is now less than that for a corresponding normalized tree where each airway is assumed to be of unit volume. Also, elasticity is shown to have only a small effect on $\Pi(s)$: it shifts the scaling regions. The shift in the scaling region can be accounted for by the fact that, for a given pressure, an avalanche will produce a larger volume in an elastic tree than in a rigid tree. Also, the maximum avalanche size (or volume) is greater for an elastic tree compared to a rigid tree with realistic dimensions due to the fact that this volume corresponds to the maximum avalanche volume in a rigid tree augmented by the additional volume due to the distension of the elastic airways. Note also that for the generation-independent distribution of $P_{i,j}$, the kink at large s disappears only due to asymmetry.

For the generation-dependent I distribution, i.e., for the case of a weak generational dependence of $P_{i,j}$, we observe a reduced scaling region. Also, for this distribution of $P_{i,j}$, the range of avalanche size is narrow for the unnormalized-rigid case as compared to the normalized and elastic cases and so we observe only one scaling region. With a stronger generational dependence of $P_{i,j}$ (the generation-dependent II distribution), the scaling behavior breaks down. Experimental data give a clear indication of scaling behavior in the distributions of the terminal airway resistances. Since our original model, which was structurally similar to the present model, provided an excellent prediction of the scaling of the resistances [6], we conclude that the distribution of the opening threshold pressures in the lung may not be essentially different from a generation-independent distribution. A stronger generational dependence of $P_{i,j}$ in the normal lung seems unlikely, as indicated by the breakdown of the scaling behavior for such a distribution of $P_{i,j}$.

B. First avalanche: Definition *A*

1. Normalized symmetric and asymmetric

Figure 3 shows the corresponding simulation results for definition *A*. In agreement with previous analytical results [11] for the generation-independent distribution, the symmetric case $\Pi(v)$ shows a single power-law behavior with an exponent of ~1.0. Also, similar to the results using definition *B*, for the generation-independent distribution and generation-dependent I distribution, asymmetry does not

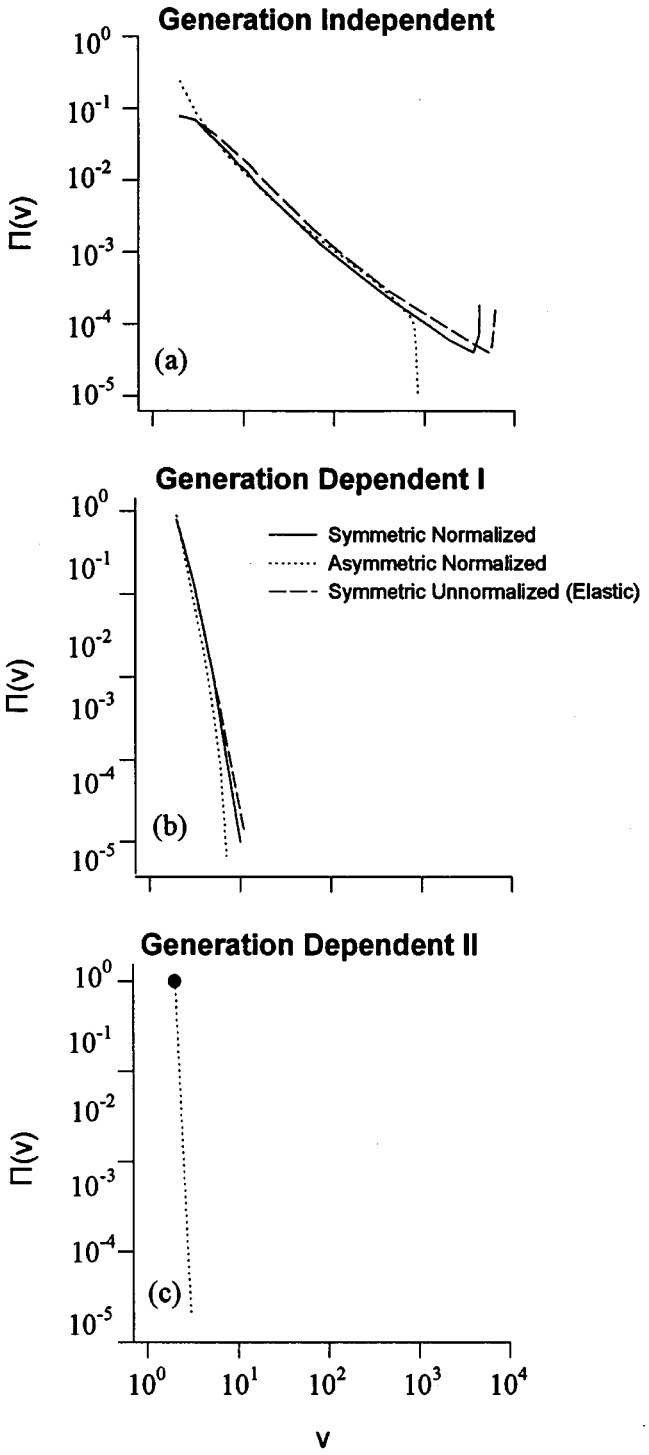

FIG. 3. Double logarithmic plots of the size distributions $\Pi(v)$ of the first avalanches for all three distributions of $P_{i,j}$, obtained by computer simulations on a Cayley tree of 12 generations for definition *A* (alveoli). The volume v is normalized to the volume of the smallest avalanche. The solid line is the size distribution for the symmetric tree. The dotted line represents the asymmetric tree, which is essentially a symmetric tree with some of its branches missing. The dashed line is the symmetric tree with realistic diameters and lengths taken from morphometric data (unnormalized) and compliant airway walls. The solid dot represents the δ function for the symmetric tree using the generation-dependent II distribution of threshold pressures.

have a significant effect on the size distributions except that for the generation-independent distribution of $P_{i,j}$ the kink disappears. In contrast, asymmetry grossly alters the slope of $\Pi(v)$ for the generation-dependent II distribution. This occurs because there is a ''gap'' between the intervals of $P_{i,j}$ of the last two generations (Fig. 1). For the symmetric tree with a generation-dependent II distribution, the threshold pressures of the last generation do not overlap with the pressures in any of the previous generations. Thus an avalanche does not occur until all the airways except the last generation airways are opened. From Fig. 1, it can be shown that for the generation-dependent II distribution, the last generation has $P_{i,j}$ distributed approximately between 0.9 and 1.0. Once all the airways except those of the last generation are open, P_E is incremented to the threshold pressure of that last-generation airway, which has the smallest opening threshold pressure. Since the probability that two or more airways in the last generation have the exact same opening threshold pressure is theoretically zero (and even for our numerical simulations, an extremely small number), we get an avalanche of size 1. Thus the size distribution for this case is a δ function at $v=1$ denoted by a filled circle in Fig. 3(c). However, in an asymmetric tree, terminal airways can exist at almost any generation of the tree and hence avalanches can occur for a wider range of pressures. Also, in the upper regions of the tree there is a significant overlap between $P_{i,j}$ of adjacent generations. Thus it is likely that there are terminal airways with smaller thresholds than their parents and, as a consequence, a single avalanche can encompass alveoli from more than one generation, resulting in a much wider range of avalanche sizes than in the case of a symmetric tree.

2. Assigning realistic airway dimensions and elasticity

Similar to the results of definition *B*, realistic dimensions and elasticity do not affect the shapes of the size distribution curves, but do cause a shift in the scaling regions (Fig. 3). In particular, elasticity extends the scaling region by a factor of 4, which is consistent with physiology that lung volume increases by a factor of 4–5 between residual volume and total lung capacity. Again, while the scaling behavior exists for the generation-independent and the generation-dependent I distributions, it is not present when the ranges of $P_{i,j}$ at consecutive generations do not overlap. In the latter case, we get avalanches of a single size and since we normalize the avalanche sizes such that the smallest size is unity, $\Pi(v)$ for this case is again a δ function at $v=1$. We emphasize that in this case asymmetry has a large influence on the distributions. Table II gives the exponents for all cases considered.

C. All avalanches

1. Exponents in the normalized tree

Figure 4 shows the effect of asymmetry on the size distributions of *all* avalanches for definition *B* in a normalized rigid tree when $P_{i,j}$ is taken from the generation-independent distribution. To distinguish between the sizes of the *first* and *all* avalanches, we denote the latter for definition *B* by *S* and for definition *A* by *V*. For the symmetric tree, there are kinks in $\Pi(S)$ spaced equally on the logarithmic axis at integral powers of 2, which can be explained as follows. Following

TABLE II. Scaling exponents of the size distributions $\Pi(v)$ of the first avalanches for definition A (alveoli) using all three distributions of $P_{i,j}$.

	Normalized		Unnormalized (elastic)	
$P_{i,j}$	Symmetric	Asymmetric	Symmetric	Asymmetric
Generation-independent	1.0±0.2	1.0±0.2	1.0±0.3	1.0±0.3
Generation-dependent I				
Generation-dependent II				

the first avalanche, the remaining unopened parts of the tree present themselves as a set of ''new'' and smaller trees, each with fewer generations than the original tree. We can consider the second avalanche to be the first avalanche in these subtrees. Since for the symmetric, generation-independent distribution case, the size of the first avalanche can take all possible values between 1 and $2^{(N+1)}-1$, the remaining ''subtrees'' of unopened airways (following the first avalanche) will present themselves as new trees with the number of generations in each tree being between 2 and $N-1$. Thus, in effect, we now have a ''first avalanche'' situation in a set of subtrees of different sizes (in the present case from size 2 to 11). Recall that $\Pi(S)$ of the first avalanches displays a kink for large avalanches (Fig. 2). Such a kink corresponding to every generation (2–12) now appears in the distribution of all avalanches $\Pi(S)$.

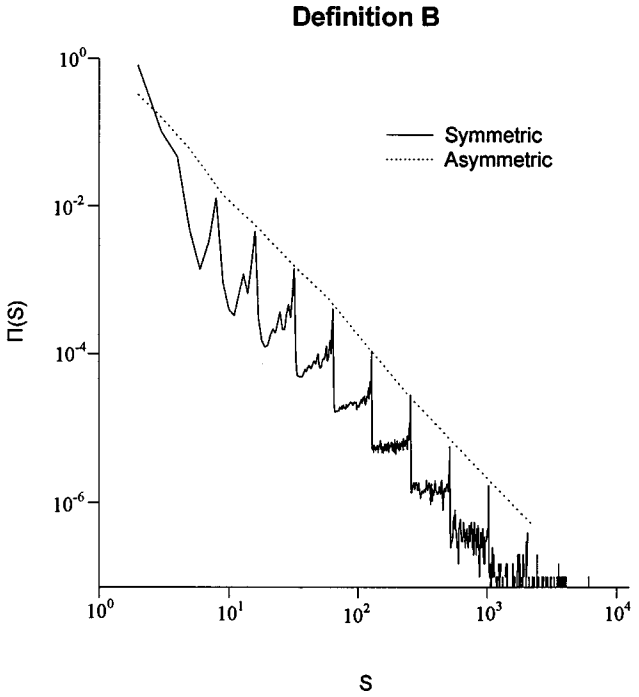

FIG. 4. Double logarithmic plots of the size distributions $\Pi(S)$ of all avalanches for definition B using the generation-independent distribution of $P_{i,j}$. Both curves are shown for the normalized-rigid 12-generation Cayley tree. The solid line is the symmetric tree with characteristic ''kinks'' at avalanche sizes of integral powers of 2. The dotted line represents the asymmetric tree.

The simulation results for definition A are very similar. The slope-2 of the line joining the tips of the kinks for the symmetric tree with the generation-independent distribution can be explained as follows. For simplicity, we first consider definition A and start with the first avalanche in an N-generation tree that has a total of 2^N alveoli. This is also the largest avalanche size in the tree, which we denote by $v(N)$. The probability that an airway has a threshold pressure less than P_E, where P_E is the external pressure applied at the root of the tree, is P_E itself. In order to get an avalanche of size $v(N)$, first all airways must open. Since in an N-generation tree there are $2^{N+1}-1$ airways, the probability that all $2^{N+1}-1$ airways will open is

$$\Pi(v(N),P_E)=P_E^{2^{(N+1)}-1}. \tag{6}$$

Since P_E itself can take any value between 0 and 1, the total probability of getting an avalanche of size $v(N)$ is

$$\Pi(v(N))=\int_0^1 P_E^{2^{(N+1)}-1}dP_E=\frac{1}{2^{N+1}}. \tag{7}$$

Thus we get a size distribution curve similar to that shown in Fig. 2 and the tip of the kink corresponding to an avalanche of size 2^N has a probability $1/2^{(N+1)}$. After each avalanche, the next avalanche can be considered as the first avalanche in a set of smaller subtrees. The next smaller subtree has $N-1$ generations. The maximum avalanche size $v(N-1)$ in these subtrees is 2^{N-1} or $v(N)/2$ and from Eq. (7) the probability is $1/2^N$. However, there are two such subtrees, so the total probability of getting an avalanche of size $v(N-1)$ is $2\times 1/2^N$ or $4\times 1/2^{(N+1)}$. So we have another size distribution curve superposed on the first, but with a kink whose tip occurs at $v(N)/2$ with probability $4/v(N)$. Thus, as the largest avalanche size is halved, the corresponding probability is quadrupled and the slope m of the line connecting the two kinks on the log-log plot is

$$m=\frac{\log[1/2^{N+1}]-\log[4/2^{N+1}]}{\log[2^N]-\log[2^{N-1}]}=-2. \tag{8}$$

For definition B, the only difference is that the largest avalanche size for an N-generation tree is $2^{N+1}-1$ which, however, does not affect the slope.

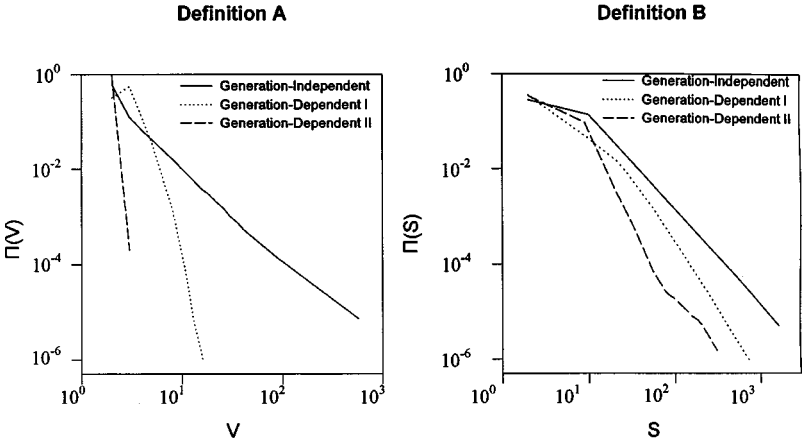

FIG. 5. Double logarithmic plots of the size distributions $\Pi(V)$ and $\Pi(S)$ of all avalanches for definitions *A* and *B*, respectively. Shown are curves for the 12-generation asymmetric Cayley tree with realistic diameters and lengths taken from morphometric data (unnormalized) and having compliant airway walls. The volume *V* is normalized to the volume of the smallest avalanche. The solid line is for the case of generation-independent distribution of $P_{i,j}$. The dotted line represents the generation-dependent II distribution of $P_{i,j}$ and the dashed line is for the case of generation-dependent I distribution of $P_{i,j}$.

2. Effect of asymmetry

As expected, asymmetry does not affect the power-law behavior. However, it removes the kinks. The reason for this is that these kinks occur at avalanche sizes of 2^k ($k=2,\ldots,N$). In an asymmetric tree, the boundaries of the symmetric subtrees blend together, the kinks disappear, and what is left is a smooth power-law curve with an exponent of $\sim$2.0. For all other cases, the results are similar to those of the first avalanche size distributions, that is, asymmetry does not affect either the shapes or the exponents of the size distributions except for definition *A* with a generation-independent distribution.

As before, simulation results for all three theshold pressure distributions indicate that while the generation-independent case and the generation-dependent I case (corresponding to weak generational dependence) preserve the power-law behavior, it is destroyed by the generation-dependent II distribution, consistent with the possibility of a generation-independent or a weakly generation-dependent distribution of threshold pressures in the lung.

3. Assigning realistic airway dimensions and elasticity

Figure 5 shows the unnormalized (i.e., realistic diameters and lengths assigned to the airways), elastic versions of the avalanche volume distributions in an asymmetric tree for definitions *A* and *B*. The effects of introducing elasticity and realistic dimensions are similar to the results obtained for the first avalanches (Fig. 4). Note, however, that with definition *B*, scaling is observed with the generation-dependent II distribution, whereas using definition *A*, scaling exists only if the distribution of thresholds is generation independent Table III gives the exponents for all cases considered.

4. Physiological implications

In order to provide a connection between our numerical results and lung physiology we calculate the pressure-volume curve of the model, which can be obtained by calculating the cumulative sum of the avalanches during inflation. In the dog lung there are 30–35 generations with airway closure occurring in the last 10–14 generations. The number of such subtrees can be several hundreds. Thus, to obtain a realistic pressure-volume curve we average 100 pressure-volume curves of the present 12-generation model.

Figure 6 shows the calculated pressure-volume curves of definition *A* using the asymmetric, unnormalized, elastic airway tree model for all three distributions of $P_{i,j}$. Here both pressure and volume are normalized to unity at the end of inspiration. For comparison, we also plot a measured pressure-volume curve of the first inflation of a degassed rabbit lung [24]. Note that no curve fitting is done. Clearly, only the curve with a generation-independent distribution matches the experimental data, strengthening our conclusion that a wide, uniformlike distribution of $P_{i,j}$ exists in the lung as opposed to a distribution with a strong generational dependence. Additionally, a curve corresponding to the equation $v=p^N$ is also plotted, where v and p are normalized

TABLE III. Scaling exponents of the size distributions $\Pi(V)$ and $\Pi(S)$ of all avalanches for definition *A* (alveoli) and definition *B* (airways), respectively, using all three distributions of $P_{i,j}$.

	Definition *A*				Definition *B*			
	Normalized		Unnormalized (elastic)		Normalized		Unnormalized (elastic)	
$P_{i,j}$	Symmetric	Asymmetric	Symmetric	Asymmetric	Symmetric	Asymmetric	Symmetric	Asymmetric
Generation-independent	2.0±0.1	2.0±0.1	2.0±0.1	2.0±0.1	2.0±0.2	2.0±0.1	2.0±0.2	2.0±0.1
Generation-dependent I					3.4±0.3	3.3±0.2	3.3±0.2	2.9±0.1
Generation-dependent II								

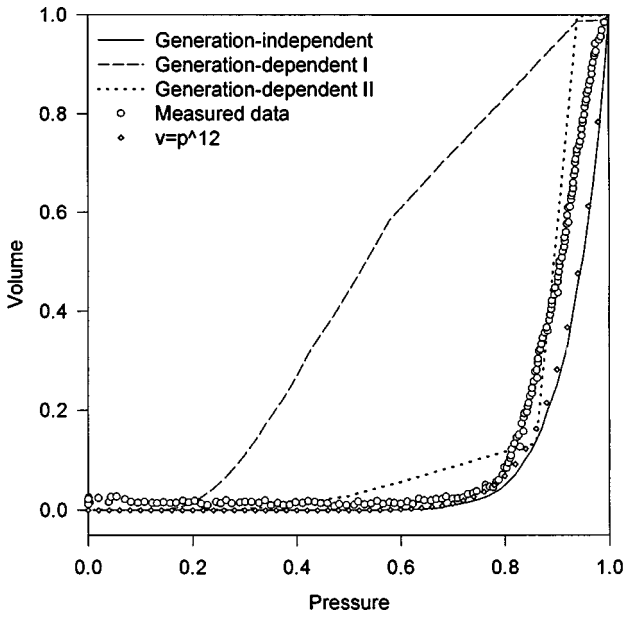

FIG. 6. Normalized pressure-volume curves simulated using the asymmetric tree with realistic diameters and lengths (unnormalized) and having compliant airway walls for all three distributions of $P_{i,j}$. Also shown, for comparison, is the plot of a *measured* pressure-volume curve of the first inflation of a degassed rabbit lung (open circles). The solid line is the simulated pressure-volume curve obtained using the generation-independent distribution of $P_{i,j}$. The dashed line represents the pressure-volume curve simulated using the generation-dependent I distribution of $P_{i,j}$. The dotted line is the pressure-volume simulation using the generation-dependent II distribution. The open diamonds are points on a curve given by the equation $v=p^{12}$, where v and p are the volume and pressure, respectively.

volume and pressure, respectively, and we choose N to be 12. This power-law relationship is obtained simply as the number of end tips reached by a branching process in a Cayley tree when the distribution of threshold pressures is generation independent. Note that the $v=p^{12}$ power law shows an excellent match with the curve corresponding to our model with a generation-independent distribution of threshold pressures. The initial gentle slope of the pressure-volume curve for the generation-dependent II distribution followed by the sudden, very steep but linear increase in volume highly resembles the pressure-volume curves obtained in a lung lavaged with a fluid of constant surface tension [25]. This suggests that in lavaged lungs this distribution is quite narrow, in contrast to normal lungs where the distribution of opening threshold pressures is wide. Such a condition can occur in respiratory distress syndrome where the lack or malfunctioning of the natural surfactant results in high surface tension forces at low lung volumes and cause an excess of airway closure. Our results suggest then that in this clinical disorder of the lung, the opening threshold pressures may be distributed in narrow intervals that depend on airway generation.

IV. CONCLUSION

We present a model of airway reopening phenomena in the lung in terms of the lung attributes asymmetry, airway and alveolar dimensions (i.e., diameters and lengths), and tissue elasticity. We perform numerical simulations of lung inflation using this model to separately study the effects of these attributes on the distribution of volumes opened by only the first avalanches and by all avalanches. Asymmetry, realistic airway and alveolar dimensions, and elasticity slightly modify the scaling region, but retain the power-law behavior as long as the distribution of threshold pressures is generation independent or slightly generation dependent. Also, for such a distribution of threshold pressures, the scaling exponent of the most realistic model (the asymmetric tree with realistic airway and alveolar dimensions and tissue elasticity) is 2, which is the value obtained both analytically using percolation theory and from simulations on a Cayley tree [11]. Thus we conclude that the power-law behavior and the scaling exponents are due to the combined effects of the tree structure, finite-size effects, and a distribution of threshold pressures that is generation independent or slightly generation dependent.

The generation-independent and generation-dependent I (i.e., the weakly generational dependent) distributions of threshold pressures both result in a scaling behavior observed experimentally. Since this scaling behavior breaks down when a strong nonoverlapping generational dependence of threshold pressures is assumed, we conclude that the distribution of threshold pressures in the normal lung at low lung volumes is most likely wide, perhaps not essentially different from a generation-independent distribution. This notion is further strengthened by our pressure-volume simulations. Also, our results are suggestive of the possibility that the present asymmetric, elastic airway tree with a generation-dependent II distribution of threshold pressures may serve as a model of lung injury or the pressure-volume behavior in respiratory distress syndrome. In the latter case, the distribution may become almost discontinuous among generations that may lead to barotrauma during inflation. Therefore, the timing and the volume delivered by a mechanical ventilator may have a significant influence on the average number of open airways in a breathing cycle. Indeed, recently Lefevre *et al.* [26] found that in lung injury, introducing ''biologic variability'' in mechanical ventilation by choosing the frequency of the ventilation from a normal distribution significantly improves gas exchange in the lung. Thus the model described in this paper may find important applications in the optimization of the ventilation strategies for individuals suffering from lung diseases with significant airway closure and alveolar collapse.

ACKNOWLEDGMENTS

We appreciate the NSF Grant No. BES-9503008 and thank OTKA 2675 and CNPq for financial support.

[1] G. Durin, G. Bertotti, and A. Magni, Fractals **3**, 351 (1995).
[2] S. Field, J. Witt, F. Nori, and X. Ling, Phys. Rev. Lett. **74**, 1206 (1995).
[3] M. P. Lilly, P. T. Finley, and R. B. Hallock, Phys. Rev. Lett. **71**, 4186 (1993). For a review see M. Sahimi, Rev. Mod. Phys. **65**, 1393 (1993).
[4] A. Petri, G. Paparo, A. Vespignani, A. Alippi, and M. Costantini, Phys. Rev. Lett. **73**, 3423 (1994).
[5] G. Gutenberg and C. F. Richter, Ann. Geophys. **9**, 1 (1956).
[6] B. Suki, A. L. Barabasi, Z. Hantos, F. Peták, and H. E. Stanley, Nature (London) **368**, 615 (1994).
[7] L. A. Engel, A. Grassino, and N. R. Anthonisen, J. Appl. Physiol. **38**, 1117 (1975).
[8] A. B. H. Crawford, D. J. Cotton, and M. Paiva, J. Appl. Physiol. **66**, 2511 (1989).
[9] F. Peták, Z. Hantos, A. Adamicza, D. R. Otis, and B. Daroczy, Eur. Respir. J. **6**, 403S (1993).
[10] D. R. Otis, Ph. D. thesis, Massachusetts Institute of Technology, 1995 (unpublished).
[11] A. L. Barabasi, S. V. Buldyrev, H. E. Stanley, and B. Suki, Phys. Rev. Lett. **76**, 2192 (1996).
[12] E. T. Naureckas, C. A. Dawson, B. S. Gerber, D. P. Gaver III, H. L. Gerber, J. H. Linehan, J. Solway, and R. W. Samsel, J. Appl. Physiol. **76**, 1372 (1994).
[13] H. Kitaoka and B. Suki, J. Appl. Physiol. **82**, 968 (1997).
[14] K. Horsfield, G. Dart, D. E. Olson, G. F. Filley, and G. Cumming, J. Appl. Physiol. **31**, 207 (1971).
[15] D. P. Gaver, R. W. Samsel, and J. Solway, J. Appl. Physiol. **69**, 74 (1990).
[16] Note that the avalanches referred to in Ref. [11] and in this paper are not to be interpreted in terms of the self-organized criticality (SOC) introduced by P. Bak, C. Tang, and K. Weisenfeld, Phys. Rev. Lett. **59**, 381 (1987). In our model, the avalanche size is controlled by P_E and the system would be critical only for a given value of $P_E = P_C$. Since P_E is swept from 0 to 1, the resulting avalanche size distribution is a power law. This mechanism has been discussed in D. Sornette, J. Phys. (France) I **4**, 209 (1994).
[17] Definition A in this paper is different from definition A of [11]. In the model of Ref. [11], an avalanche of size 0 is possible [this occurs when P_E is equal to or greater than $P_{0,0}$, causing airway (0,0) and possibly other airways to open, but not sufficient to cause the avalanche to reach at least one alveolus]. In this paper, an avalanche of size 0 is forbidden. If $P_E \geqslant P_{0,0}$ does not open any alveolus, then P_E is further increased until at least one alveolus opens. Consequently, for small avalanche size v, the size distributions for definition A in this paper differ from those of Ref. [11]. However, for large avalanches, the main contribution is made when $P_E > 0.5$, in which case the Cayley tree is percolating and at least one alveolus is open. Thus, for large avalanches, both definitions give similar results.
[18] A. Bunde and S. Havlin, in *Fractals and Disordered Systems*, edited by A. Bunde and S. Havlin, 2nd ed. (Springer-Verlag, Berlin, 1996).
[19] J. Essam, Rep. Prog. Phys. **43**, 833 (1980).
[20] H. C. Yeh, G. M. Schum, and M. J. Duggan, Anat. Rec. **195**, 483 (1979).
[21] O. G. Raabe, H. C. Yeh, H. M. Schum, and R. F. Phalen, Lovelace Foundation for Medical Education and Research Report No. LF-53, 1976 (unpublished).
[22] R. K. Lambert, T. A. Wilson, R. E. Hyatt, and J. R. Rodart, J. Appl. Physiol. **52**, 44 (1982).
[23] E. Salazar and J. H. Knowles, J. Appl. Physiol. **19**, 97 (1964).
[24] B. Suki, J. S. Andrade, Jr., M. F. Coughlin, D. Stamenović, H. E. Stanley, M. Sujeer, and S. Zapperi (unpublished).
[25] J. C. Smith and D. Stamenović, J. Appl. Physiol. **60**, 1341 (1986).
[26] G. R. Lefevre, S. E. Kowalski, L. G. Girling, D. B. Thiessen, and W. A. C. Mutch, Am. J. Respir. Crit. Care Med. **154**, 1567 (1996).